

Synchrotron x-rays and condensed matter/Rayonnement X synchrotron et matière condensée

## High energy X-ray micro-optics

Anatoly Snigirev<sup>\*</sup>, Irina Snigireva

European Synchrotron Radiation Facility ESRF, 38043 Grenoble, France

Available online 18 April 2008

### Abstract

A tremendous progress in X-ray optics development was made in the past decade. Progress has been driven by the unique properties of X-ray beams produced by third generation synchrotron sources. The very low emittance coupled with high brilliance allows one to develop efficient focusing devices for new X-ray microscopy techniques. This article provides an overview of the state-of-the-art in micro-focusing optics and methods for hard X-rays. The main emphasis is put on those methods which aim to produce submicron and nanometer resolution. These methods fall into three broad categories: reflective, refractive and diffractive optics.

The basic principles and recent achievements are discussed for all optical devices. *To cite this article: A. Snigirev, I. Snigireva, C. R. Physique 9 (2008).*

© 2008 Académie des sciences. Published by Elsevier Masson SAS. All rights reserved.

### Résumé

**Micro-optique pour rayons X de haute énergie.** Pendant la dernière décennie, des progrès énormes ont été accomplis dans le domaine de l'optique des rayons X. Ces progrès découlent des propriétés uniques des faisceaux X produits par les sources synchrotron de troisième génération, dont la faible émittance, couplée à une brillance élevée, permet le développement de dispositifs de focalisation efficaces pour de nouvelles techniques de microscopie X. Cet article donne un aperçu de l'état de l'art des optiques microfocalisantes et des méthodes pour les rayons X durs. L'accent est mis sur les méthodes visant à produire une résolution submicrométrique, voire nanométrique. Ces méthodes se rangent dans trois grandes catégories : réflexion, réfraction et diffraction.

Nous présentons les principes de base et des résultats récents pour chaque dispositif optique. *Pour citer cet article : A. Snigirev, I. Snigireva, C. R. Physique 9 (2008).*

© 2008 Académie des sciences. Published by Elsevier Masson SAS. All rights reserved.

**Keywords:** X-ray micro-optics; Kirkpatrick–Baez mirrors; Fresnel zone plates; Waveguides; Capillaries; Refractive lenses

**Mots-clés :** Micro-optique pour rayons X ; Miroirs Kirkpatrick–Baez ; Réseau zoné de Fresnel ; Guide d'ondes ; Tube capillaire ; Objectif réfractif




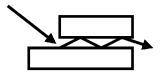
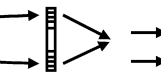
## 1. Introduction

The advent of third generation storage rings like ESRF, APS and SPring-8 with beams of high brilliance, low divergence and high coherence allows efficient X-ray focusing and imaging. The article is intended to provide a summary of micro-focusing optics and methods for hard X-rays. The hard X-ray region is taken as extending from about several

<sup>\*</sup> Corresponding author.

E-mail address: [snigirev@esrf.fr](mailto:snigirev@esrf.fr) (A. Snigirev).

Table 1  
Microfocusing optics for hard X-rays

Reflective				Diffractive	Refractive		
Kirkpatrick–Baez systems		Capillaries		Waveguides	Fresnel zone plates	Refractive lenses	
mirrors	multilayers	multi-bounce	one-bounce				
Kirkpatrick Baez, 1948	Undewood Barbee, 1986	Kreger, 1948	Balaic, 1995	Feng et al., 1993	Baez, 1952	Snigirev et al., 1996	
							
$E$	<20 keV	<80 keV	<20 keV	<20 keV	<30 keV	<1 MeV	
$\Delta E/E$	white beam	$10^{-2}$	white beam	$10^{-3}$	$10^{-3}$	$10^{-3}$	
$\Delta$	25 nm	41 nm	50 nm	250 nm	$40 \times 25 \text{ nm}^2$	30 nm	
	[1]	[2]	[3]	[4]	[5]	[6]	
						[7]	

$E$  – energy range,  $\Delta E/E$  – energy band width,  $\Delta$  – best measured resolution.

keV ( $\sim 4$  keV) to gamma rays with several hundred keV ( $\sim 100$  keV) provided by synchrotron radiation sources. The main emphasis will be on those methods which aim to produce sub-micron and nanometer resolution. These methods fall into three broad categories: reflective, refractive and diffractive optics. The basic principles and recent achievements will be discussed for all optical devices. The report covers the latest status of reflective optics including mirrors and multilayers, capillaries and waveguides. Special attention will be given to the successful development of Kirkpatrick–Baez systems, providing submicro- and nanometer focusing in two dimensions. We will review the basic principles and state of the art of diffractive optics, such as Fresnel zone plates. Improvement of the spatial resolution without loss of efficiency is difficult and incremental due to the fabrication challenges posed by the combination of small outermost zone width and high aspect ratios. Particular attention will be given to the recent invention of refractive optics. Refractive optics is a rapidly emerging option for focusing high energy synchrotron radiation from micro- to nano-meter dimensions. These devices are simple to align, allow a good working distance between the optics and the sample, and are becoming standard elements in synchrotron beamline instrumentation in general, and in high energy X-ray microscopy, in particular. The small source size and low divergence of 3d generation synchrotron radiation sources give rise to tremendous advances in the development of different types of microfocusing optics based on reflection, diffraction and refraction phenomena. All available microfocusing devices for hard X rays are presented in Table 1. The best resolution for all the presented optical systems overcomes the 100 nm limit.

## 2. Kirkpatrick–Baez systems

In the X-ray regime, conventional mirrors have to be used, applying the total external reflection geometry. At X-ray wavelengths the index of refraction  $n \sim 1 - \delta + i\beta$  is less than 1, but the deviation is proportional to electron density. Because  $n < 1$ , X-rays bend away from the normal when entering dense materials, whereas visible light bends towards the normal. High reflectivity occurs when the glancing angle is below a critical angle  $\theta_c < \sqrt{2\delta}$ . To reduce the astigmatism, Kirkpatrick and Baez proposed to use two spherical or cylindrical mirrors in a crossed configuration [8]. Fig. 1 shows a geometrical arrangement of such a so-called Kirkpatrick–Baez system (KB mirrors). To enhance the reflectivity, multilayer mirrors, where the refractive index varies periodically with depth, can be used. Multilayer mirrors are formed by depositing alternating layers of two materials of different refractive index that form long-term stable interfaces. Typically the two materials are of alternating high and low atomic number ( $Z_0$ ) in order to maximize the difference in electron density. The coatings are largely amorphous within individual layers, and reflection conforms to Bragg's law for a periodicity  $d$  equal to the thickness of one bilayer pair. The weak radiation reflected at the interfaces of the multilayer is superimposed coherently and in phase, and can give a considerably increased reflectivity.

Reflecting focusing systems can be either static, with mirrors polished according to the proper figure optimized for a given incidence angle and focus, or they can be dynamic, with actuators bending flat mirrors into the elliptical shapes, as required by the experiment. Today, as a result of improved techniques for developing highly finished and perfect

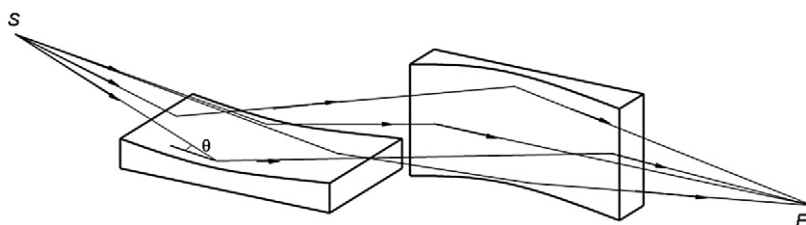


Fig. 1. Schematic view of two mirrors Kirkpatrick–Baez system.  $\theta$  is the mirror incidence angle,  $S$  is the source and  $F$  is focus.

surfaces, ellipsoidal and paraboloidal mirrors can be manufactured to a high degree of perfection, and focusing down to 100 nm spot size is achievable with KB systems.

Reflecting mirrors are able to focus X-rays over large energy range, whereas Bragg reflecting multilayer mirrors only focus a small energy bandwidth ( $\sim 1\text{--}2\%$ ). As, within a given energy interval, the optical properties for total reflecting optics are independent of the X-ray wavelength, the focal spot is retained while tuning the energy. Therefore, experiments requiring energy tuning, like spectroscopy, can be performed without any readjustment of the optics. However, the disadvantage of grazing incidence optic is low acceptance and it is mostly used for scanning microscopes. KB systems at the ESRF are based on dynamical bending systems where initially flat, superpolished plates are used [2,9]. The obvious advantage of dynamical bending is that it permits one to tune the focusing conditions. Newly developed surface preparation techniques and a computer control alignment procedure allow one to achieve a spot size of 41 nm using 24 keV [2].

Although KB mirrors with benders are flexible in adjusting the focal length, the benders are bulky. In addition, in view of applying of nanofocusing systems the stability achieved is not sufficient to support long time scanning experiments and the efficiency of microfocusing is affected by dynamic stability. For these reasons static KB systems were chosen at the Spring-8 [1,10,11] and APS [12,13]. For the Spring-8 KB system in mirror fabrication, plasma chemical vaporization machining (PCVM) is employed for rough figuring and elastic emission machining (EEM) is used for final figuring and surface super smoothing. These methods do not cause mechanical damage to processed surfaces because their removal mechanism is based on chemical reactions. By combining these two methods, accurate surfaces without precedent can be created with 0.1 nm controllability and 0.3 mm spatial resolution. Typically, the surfaces after the final figuring were coated with a 50 nm Pt layer using an electron evaporation method. The KB system was tested at the 1-km-long beamline BL29XUL at Spring-8 using a 15 keV monochromatic beam. A focal spot of 25 nm was measured [1]. The proposed KB device employing precisely figured mirrors is promising, not only on the basis of focusing performance, but also capabilities for user-friendly instrumentation.

Elliptical surfaces can be obtained by differential coating a flat or a spherical mirror with a continuously variable amount of gold. This idea was proposed more than 60 years ago and recently was revised at the APS [12,13]. Profile coatings have been applied on both cylindrical and flat Si substrates to make the desired elliptical shape. In a profile-coating process, the sputter source power is kept constant, while the substrate is passed over a contoured mask at a constant speed to obtain a desired profile along the direction perpendicular to the substrate-moving direction. A KB mirror pair was made using Au as a coating material was recently tested at the APS and X-ray results showed a focused spot size of  $80\text{ nm} \times 70\text{ nm}$  [13].

### 3. Capillaries

Similar to reflective mirrors, monocapillary optics relies on total external reflection of the X-rays from the internal surface of the tube to transport X-rays. Typical glass materials that have been used to fabricate capillary optics are borosilicate, lead based, and silica glasses. For hard X-rays the typical values for critical angles are 0.1 to 10 mrad. The simplest form of a capillary is a straight (cylindrical) glass tube; have first been used in the 1950s to guide X-rays from the source point to a distant sample. This leads to an effective reduction of the source sample distance, and thus to an increase in flux on the sample. The next step was to use tapered capillaries not only to guide, but moreover to squeeze the X-rays to a very small spot [14,15] (see Fig. 2(a)).

Tapered capillaries have shown nanofocusing capabilities already more than 10 years ago [3]; however, no appreciable progress of using such simple devices for nanobeams has been made so far since that time. The problems are well understood and consist of significant losses in the multireflection process and almost zero-working distance,

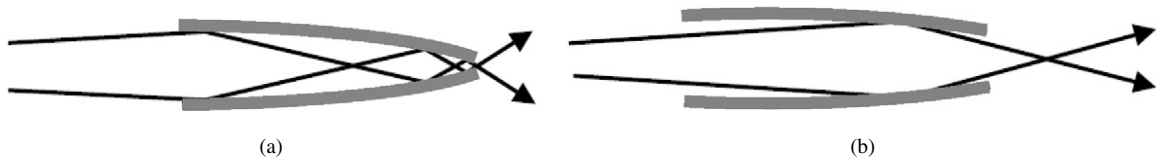


Fig. 2. Schematic of tapered multi-bounce (a) and single bounce (b) capillaries.

which substantially limits practical applications of capillaries in X-ray microscopy. On the contrary, single-bounced capillaries proposed by [16] show a great potential in developing nanofocusing devices (Fig. 2(b)). Parabolic and elliptical capillaries have a large focal distance and very high reflectivity [17,18]. In a typical process the predetermined capillary profile is achieved by “pulling” of an originally straight uniform glass tube with accurate control of mechanical movements and heating parameters. Unfortunately, due to some unavoidable factors i.e. surface slope errors of the original glass tube and non-uniform mechanical movement, it is difficult to reliably achieve elliptical or parabolic shapes with the desired low-figure errors. State-of-the-art technology allows one to produce a capillary with 70 microradian slope errors [17]. Obviously such slope errors limit the resolution of the optic to a size of about 10  $\mu\text{m}$ .

To overcome these problems it was proposed to use a small elliptical capillary made by a stationary pulling technique, where the elliptical shape is achieved by stretching an air bubble inside a glass fiber [19]. It appears that this approach shows a better quality surface as compared to the glass tube pulling process. For best performance of the ellipsoidal capillary a Fresnel zone plate was used as a first microfocusing element to produce a demagnified micrometer image of the source and then the elliptical capillary makes a last final compression of the beam down to 250–500 nm [4]. In general, the two step-focusing setup provides three important benefits: (i) it significantly improves the flux by increasing the overall acceptance of the optical system; (ii) it allows optimal aberration-free focusing by the elliptical capillary surface, and (iii) it considerably minimizes the influence of slope errors. For practical applications, off-axis illumination of the capillary by small prefocused beam eliminates the beam transmitted through the exit aperture and makes for an easy implementation of a beamstop. The proposed approach allows one to shorten a small capillary further down to 5–10 mm, making it easy to align and operate. Use of short capillaries might open the possibilities of coating the inside of capillaries with metal films such as platinum or gold. Finally, the single-bounce ellipsoidal capillaries are very attractive for X-ray nano-beam techniques because they are so simple and have the potential to be reproduced inexpensively.

#### 4. Waveguides

An X-ray planar waveguide is a thin film resonator in which a low absorbing material is enclosed between two metal layers with smaller refractive index [20]. For particular grazing incidence angles, a resonator effect takes place inside the resonator film. Schematic representation of thin film waveguide is shown in Fig. 3. The beam is compressed in one direction and the trapped wave emerges from the end of the waveguide with enhanced intensity. In the direction of beam compression, the beam leaves the waveguide with the vertical size limited by the resonator layer thickness, which can be as small as 100 nm [21]. The cover layer and under layer can also be constituted of the same material. To date, X-ray waveguide optics have been exclusively one-dimensional, whereas most nanobeam applications require two-dimensional point beams. Recently, in [5,22], the first proof of principle that resonant beam coupling can be realized in two dimensions was reported. Also, although the reported hard X-ray beam with a cross section of  $25 \times 47 \text{ nm}^2$  (FWHM) is impressive, many technological improvements will be required before this device can be used as an efficient X-ray point source.

#### 5. Fresnel zone plates

The focusing properties of zone plates were first discussed in the latter part of the 19th century, and Baez originally suggested their use as X-ray optical elements in 1952 [23]. In their most common form, this is circular diffraction grating that works as a lens for monochromatic light. A Fresnel zone plate consists of a series of concentric rings of radius  $r_n^2 = n\lambda F$  and the rings become narrower at larger radii until the last, finest zone of width  $\Delta r_n$  is reached (Fig. 4). Linear, square, elliptical zone plates have also been considered, but only circular and, to a lesser extent, linear and elliptical forms have generally been used. The focusing capability is based on constructive interference

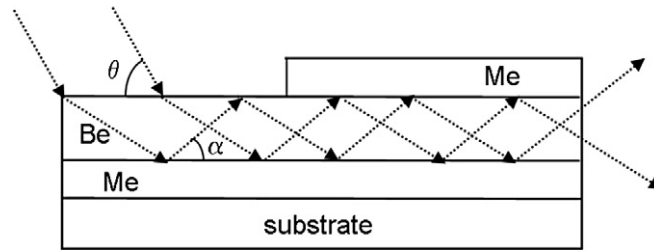


Fig. 3. Schematic design of the waveguide structure.  $\theta$  is the incidence angle on the waveguide surface; incidence angle  $\alpha$  on the interior metal surface of the waveguide differs from the  $\theta$  due to the refraction on the film.

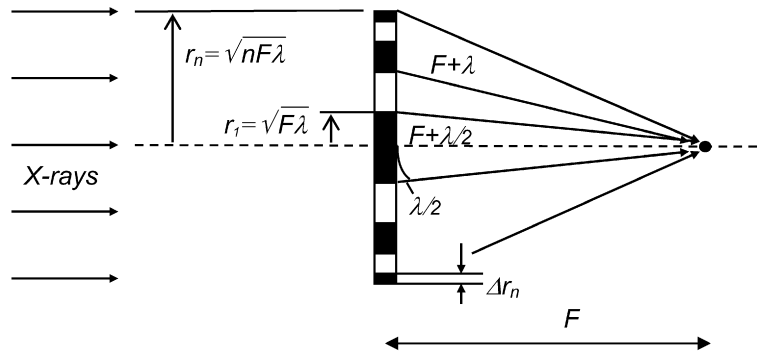


Fig. 4. Fresnel zone plate geometry.

of the wavefront modified by passage through the zone plate. The wavefront modification is obtained through the introduction of a relative change in amplitude or phase in the beams emerging from two neighboring zones. A zone plate is called an amplitude zone plate if the focusing results from different absorption between two neighboring zones. It is called a phase zone plate if the phase change upon transmission through a zone is the mechanism for focusing

Using state-of-the-art lithographic technologies, zone plates with a last or outermost ring width of less than 20 nm can currently be fabricated. If illuminated with an X-ray beam whose spatial coherence length is equal to or greater than the diameter of the zone plate, a diffraction-limited focus can be obtained. The efficiency of zone plates, i.e. the fraction of the incident photons diffracted into the focal spot, depends on the phase shift and attenuation introduced by the FZP structures. In the soft X-ray region, zone plate efficiency is limited to about 15% due to photoelectric absorption. For X-ray energies greater than 4 keV, it is possible to produce phase zone plates with focusing efficiencies close to 40%.

The efficiency of binary FZP reaches its maximum value when the structure height is chosen to introduce a phase shift of  $\pi$ . As a phase shift generally decreases with increasing photon energy, high and higher structures are required to provide useful efficiency values for harder X-rays. For example, appropriate zone thickness for 10 keV X-rays is estimated to be about 2  $\mu\text{m}$  even for high density material like gold or tantalum. The resulting extreme aspect ratios (height/width of finest zone), are the reason why FZPs for hard X-rays cannot be made with zone width as small as those for soft X-rays. In fact, FZPs have only very rarely been used for energies beyond 12 keV.

As it was mentioned above, the spatial resolution of a zone plate is determined by the outermost zone width  $\Delta r_n$ ; manufacturing techniques must be capable of delivering small line widths over large areas (to give apertures as large as possible) with zone thicknesses of the correct values to give good diffraction efficiencies. The accuracy of the technique must be sufficient to allow zone boundaries to within about one-third of the outer zone width and to date two main approaches are basically used to achieve this. The more frequently used technique for FZP manufacturing is based on semiconductor MEMS (micro-electro-mechanical systems) technology and is similar to the technique employed in the manufacture of microcircuits. This technique is based on lithography methods with consecutive deep pattern transfer. As far as the optical lithography is limited by 0.2 micrometer resolution mainly electron beam

lithography is used for manufacturing high resolution zone plates. Currently the best performing zone plate lenses for multi-keV X-rays in terms of resolution and efficiency are fabricated by means of a deep pattern transfer process.

To reproduce the zone plate structure in a suitable material, lithographically-based techniques can be subdivided in two main patterns transfer methods: wet or reactive ion etching and electrochemical deposition (electroplating). The first method can be applied to metals (Ta FZP) [24–27] and semiconductors (Si FZP) [28,29], whether electroplating can be applied only for metals and typically uses gold [30–32]. To date, typical aspect ratios achieved using e-beam lithography and consecutive pattern transfer for 100 nm structures are on the order of 10:1–15:1. Recently microfabrication MEMS technology was successfully used to produce Si-FZP for hard X-rays and using reactive ion etching of Si aspect-ratio about 40–50 has been demonstrated for modest resolution zone plates with 400 nm outermost zone [33].

To overcome the aspect-ratio limitation, one can attempt a multiple zone plate setup. Two stacked zone plates made of Si can focus 50 keV X-rays with 35% efficiency [33]. The developed technique will be used for the future development of Fresnel optics with higher resolution and can be extended to “thin” nanofocusing FZPs. The sputtered-sliced FZP method was proposed [34,35] to produce thicker FZP. In this technique, two different materials of heavy and light elements are alternately deposited on a rotating gold wire core to give concentric multilayer structure. Another way of solving aspect-ratio problem was proposed recently by [29], applying inclined geometry for a linear zone plate.

It is clear, however, the focusing properties of all binary ZPs developed for X-ray applications are far from those of an ideal lens because a significant fraction of incident photons was delivered to the undiffracted zero-order beam and to diffraction orders other than the primary first order. For instance, although in principle the undiffracted zero-order beam for an ideal phase zone plate is completely reduced to zero, about 60% of the incident beam is still delivered to other unwanted orders. The first zone plate with a blazed zone profile was manufactured at Wisconsin and tested at the APS using 8 keV X-rays showing 45% efficiency for linear and 39% efficiency for circular ZPs, respectively [36]. Later 55% efficiency for the nickel circular zone plate at 7 keV was achieved at the ESRF [37]. In practice, still, production of high-resolution zone plates with a blazed profile is very complicated and expensive and a resolution better than 0.5  $\mu\text{m}$  has never been shown for these devices.

A novel approach for high-resolution X-ray focusing, a Multilayer Laue Lens (MLL) was proposed [6,38]. The MLL concept is a system of two crossed linear zone plates, manufactured by deposition techniques. The approach involves deposition of a multilayer with a graded period, sectioning it to the appropriate thickness, assembling the sections at the optimum angle, and using it in Laue geometry for focusing. The approach is particularly well suited for high-resolution focusing optics for use at high photon energy. A 30 nm resolution was achieved with MLL FZPs [6].

## 6. Refractive optics

Refractive lenses made of glass are among the most widely used optical components for visible light, with the wide spectrum of applications in focusing and imaging. Refractive lenses for X-rays were considered unfeasible for a long time due to the weak refraction and strong absorption. However, in 1996 it was shown that focusing by X-ray lenses is possible [39]. As it was mentioned earlier, since the  $(1 - \delta)$  in the index of refraction is smaller than 1, lenses must have a concave shape [39,40]. In order to obtain a focal length  $F$  in the range of one meter many single lenses have to be stacked behind each other to form a compound refractive lens (CRL), as shown in Fig. 5. Fabricating the lenses from low-Z materials like Li, Be, B, C, and Al minimizes the problems associated with absorption. The focal length of such CRL  $N$  individual biconcave lenses is  $F = R/2N\delta$ , where  $R$  is the radius of curvature.

The first lenses consisted of a row of holes, about 1 mm in diameter, drilled in a material such as Al or Be. Two of these lenses in a crossed geometry are able to focus the X-ray beam to a spot size of a few microns. Soon after this first successful experimental demonstration it was understood that refractive lenses can be used as a condensers or collimators with relatively long focal distances. Be, Graphite and Al lenses were installed at the front-ends about 24 m from the source at various beamlines [41]. The typical front-end CRL consists of a series of cylindrical holes drilled into a material. By varying the number of holes and their radius, it is possible to fine-tune the focal length of the lenses, making them a very useful device not only to focus but also to collimate a divergent X-ray beam [42].

Al and Be parabolic refractive lenses were developed in collaboration with Aachen University [43,44]. These allow for focusing in both directions, free of spherical aberrations and other distortions. Parabolic refractive lenses can be used to focus hard X-rays in both directions in the range from about 5 keV to about 200 keV. They can be used like glass lenses are used for visible light providing the resolution in the order of 300–500 nm [43]. Their main

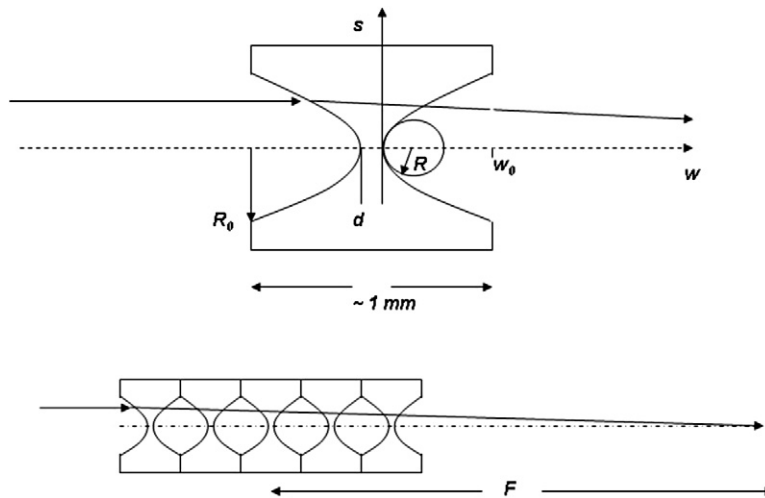


Fig. 5. Parabolic compound refractive lens (CRL). The individual lenses are stacked behind one another to form a CRL.

applications are in micro- and nano-focusing, in imaging by absorption and phase contrast [45]. In combination with tomography they allow 3D imaging of opaque media with sub-micrometer resolution [46]. The Be and Al lenses for two-dimensional focusing are now extensively used as a standard tool in experiments. A number of new applications using hard X-rays above 40 keV such as surface and interface scattering are under extensive development [47].

Unfortunately, since the index of refraction depends on the X-ray energy, refractive lenses are chromatic and this substantially limits their applicability. Therefore there is a strong demand for the development of energy tunable refractive optical systems when X-ray energy can be tuned in a reasonable range without changing the beam position on the sample. In case of saw-tooth refractive lenses one can easily tune the energy by changing the gap between lenses [48,49]. As concerns 2D parabolic lenses [43], this problem can be solved using a so called X-ray *transfocator* – a lens assembly whose focal length can be continuously adjusted by the mechanical movement of one or more groups of individual parabolic lenses [50]. Typically the transfocator consists of several cylindrical cartridges containing 2, 4, 8, 16, 32, 64, etc. Al or Be parabolic lenses. Pneumatic actuators can be used to bring cartridges in and out of the beam independently providing collimation or focusing at a desired distance downstream. Transfocators with changeable number of lenses are being installed at different beamlines at the ESRF.

Recently, microelectronics planar fabrication technology has been applied to obtain silicon-based devices [51–55]. One-dimensional focusing, parabolic refractive lenses have been manufactured in collaboration with the Institute of Microelectronics Technology (Chernogolovka, Russia) and the Dortmund University using lithography and highly anisotropic plasma etching techniques. This type of planar lenses is well suited for high-resolution diffraction experiments including standing wave technique [53]. It was proposed to manufacture sets of compound planar parabolic refractive lenses as integrated lens systems (ILS) [54]. ILS consists of arrays of compound refractive lenses aligned in parallel. One lens array in ILS by itself is optimized for certain energy and a number of arrays taken together allow one to cover a considerable energy range. All lenses in ILS have a fixed focal distance that was achieved by varying the numbers of individual lenses in each compound refractive lens. To choose the desirable working energy, one can switch from one lens array to another by parallel displacement of ILS in vertical direction. Using Si-planar lenses focus spot about 50 nm has been achieved [7]. Driven by the requirements of new 100 m-long beamlines at the ESRF Si planar parabolic lenses were designed and fabricated (Fig. 6). They have a short focal distance in the energy range of 10 and 100 keV. The resolution below 200 nm was measured in the energy region of 15–80 keV. The best resolution of 150 nm was demonstrated at 50 keV energy [55].

The applicability of Si or Al lenses at energies above 100 keV is limited by the physical size of the lens assembly because the number of individual lenses required to produce a reasonable focal distance grows quickly with energy. Using denser lens materials, such as nickel, the number of lenses needed, can be drastically reduced. While the absorption in nickel is still tolerable, its density and thus its refraction are higher compared to the low Z materials used. Nickel is the most promising since it is radiation and corrosion stable and, what is more important, it is the one of the best material for electroplating. A LIGA technology including deep X-ray lithography and electroplating was

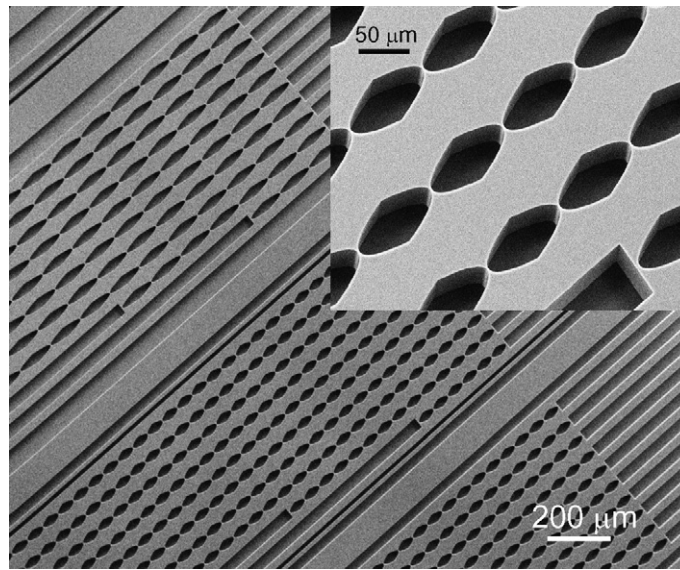


Fig. 6. SEM image of the Si planar refractive lens. Insert shows more detailed view of 50  $\mu\text{m}$  aperture lenses.

used to manufacture Ni planar refractive lenses for X-ray energies from 40 to 220 keV. Sub micrometer focusing was measured in the energy range from 40 to 150 keV [56].

Recently, holographic or kinoform optical elements with the combination of refractive and diffractive properties were manufactured [51,52]. In these refractive lenses passive parts of the material that cause multiples of  $2\pi$  in phase shift are removed, thereby reducing absorption. With this method drawbacks of purely diffractive or refractive elements are eliminated and advantages like high transmission, absence of zero-order, and high efficiency are combined. Ni kinoform lenses made by LIGA focused 212 keV X-rays to a focal line 5 microns wide with a 10-fold gain [56]. The ability to manipulate the local amplitude and phase of the incoming wave opens the perspective to make a new class of beamshaping X-ray optics for coherent synchrotron radiation.

## 7. Conclusion

The foregoing overview shows the tremendous development in the possibilities for X-ray focusing that now allow the construction of powerful microscopy instruments at synchrotron radiation beamlines. In conclusion, we would like to compare different focusing systems. Firstly we should mention that reflective, diffractive and refractive micro-optics have the following features in common. All three types are under intensive development at all new synchrotron radiation facilities and they are becoming commercially available. They are used as a standard BL instrumentation at the beamlines. All three types show nano-focusing capabilities.

KB mirrors have intrinsic advantage compared to other techniques, such as Fresnel zone plates and refractive optics: non-dispersive or broadband focusing. In case of dynamic KB systems sophisticated bending techniques have been developed to bend mirrors to achieve the desired elliptical shape for micro- and nano-focusing. Mirrors with benders are flexible in adjusting the focal length, but the benders are bulky. Monolithic or static KB systems are much easier to use if the desired elliptical surface profile can be fabricated.

FZP and refractive optics, being in-line optics, have certain advantages versus KB-systems. On-axis optics do not change the beam direction, providing easy alignment and operation. They can be easily implemented at any beamline (including non-specific beamlines). In case of nanofocusing geometry FZP and CRL should have greater clearance from the optics to the sample. FZP elements have attractive features in that they are very compact and easy to use. The alignment mechanics requires basically only two orthogonal translations (XZ) and therefore they can be easily used at any non-specific beamline. Si FZPs are compatible with multilayer monochromatic and “pink” beams, because of high radiation and temperature stability. The advantages of CRLs are: they are very robust and small, the focal length and size are adjustable by adding or removing individual lenses and the lenses can withstand high heatload. The lens aperture can range from few microns to few millimeters. Their focal distances can range from a few millimeters to



tens of meters. What is more, CRLs can cover energy range from 4 keV to 200 keV and higher. Compared to mirrors, refractive lenses are about a factor of 1000 less sensitive to surface roughness. This is an important aspect in the production process of the lenses. It turned out that surface roughness plays no role in imaging by refractive X-ray lenses.

Comparing different optics, it is of great interest to consider what is a physical limit to efficient focusing of hard X-rays. It was found that mirrors and waveguides have a numerical aperture limited by critical angle of total reflection and the ultimate resolution limit is 10 nm [57], while for refractive optics this limit is slightly lower and is 2 nm might be achievable [58]. Unlike reflective and refractive optics zone plates can focus X-rays below 1 nm [59,60]. In this case, complex multilayer zone plates have to be manufactured and Bragg conditions have to be fulfilled for the outermost zones. As for conventional zone plates, it can be estimated that the practical limit for hard X-ray zone plates using current pattern transfer technology is around 20–30 nm (structures height  $\cong$  1  $\mu$ m). It is believed that using higher diffraction orders, such as 3rd diffraction order, it is possible to achieve sub-10 nm resolution X-ray imaging.

Use of micro-optics along with high brilliance and spatial coherence of the X-ray beam provided by the third generation synchrotron radiation sources makes possible to realize high energy X-ray microscopy as a combination of diffraction, fluorescence and imaging techniques. The availability of these techniques is opening up research opportunities for a broad range of disciplines including material science, biology, environment and geosciences.

## References

- [1] H. Mimura, H. Yumoto, S. Matsuyama, Y. Sano, K. Yamamura, Y. Mori, M. Yabashi, Y. Nishino, K. Tamasaku, T. Ishikawa, K. Yamauchi, *Appl. Phys. Lett.* 90 (2007) 051903.
- [2] O. Hignette, P. Cloetens, C. Morawe, C. Borel, W. Ludwig, P. Bernard, A. Rommeveaux, S. Bohic, *AIP Conf. Proc.* 879 (2007) 792–799.
- [3] D.H. Bilderback, S.A. Hoffman, D.J. Thiel, *Science* 263 (1994) 201–203.
- [4] A. Snigirev, A. Bjeoumikhov, A. Erko, I. Snigireva, M. Grigoriev, V. Yunkin, M. Erko, S. Bjeoumikhova, *J. Synchrotron Rad.* 14 (2007) 326–330.
- [5] A. Jarre, C. Fuhse, C. Ollinger, J. Seeger, R. Tucoulou, T. Salditt, *Phys. Rev. Lett.* 94 (2005) 074801.
- [6] H.C. Kang, J. Maser, G.B. Stephenson, C. Liu, R. Conley, A.T. Macrander, S. Vogt, *Phys. Rev. Lett.* 96 (2006) 127401.
- [7] C.G. Schroer, O. Kurapova, J. Patommel, P. Boye, J. Feldkamp, B. Lengeler, M. Burghammer, C. Riekkel, L. Vincze, A. van der Hart, M. Kuchler, *Appl. Phys. Lett.* 87 (2005) 124103.
- [8] P. Kirkpatrick, A.V. Baez, *J. Opt. Soc. Am.* 38 (1948) 766–774.
- [9] O. Hignette, P. Cloetens, G. Rostaing, P. Bernard, C. Morawe, *Rev. Sci. Instrum.* 76 (2005) 063709.
- [10] K. Yamauchi, K. Yamamura, H. Mimura, Y. Sano, A. Saito, A. Souvorov, M. Yabashi, K. Tamasaku, T. Ishikawa, Y. Mori, *J. Synchrotron Rad.* 9 (2002) 313–316.
- [11] H. Yumoto, H. Mimura, S. Matsuyama, S. Handa, Y. Sano, M. Yabashi, Y. Nishino, K. Tamasaku, T. Ishikawa, K. Yamauchi, *Rev. Sci. Instrum.* 77 (2006) 063712.
- [12] G.E. Ice, J.S. Chung, J. Tischler, A. Lunt, L. Assoufid, *Rev. Sci. Instrum.* 71 (2000) 2635–2639.
- [13] W. Liu, G.E. Ice, Z. Tischler, A. Khonsary, C. Liu, L. Assoufid, A.T. Macrander, *Rev. Sci. Instrum.* 76 (2005) 113701.
- [14] D.R. Kreger, *Rec. Trav. Bot. Neerlandais* 41 (1948) 603.
- [15] E.A. Stern, Z. Kalman, A. Lewis, K. Lieberman, *Appl. Opt.* 27 (1988) 5135.
- [16] D.X. Balaic, K.A. Nugent, Z. Barnea, R. Garret, S.W. Wilkins, *J. Synchrotron Rad.* 2 (1995) 296–299.
- [17] R. Huang, D. Bilderback, *J. Synchrotron Rad.* 13 (2006) 74–84.
- [18] A. Bjeoumikhov, S. Bjeoumikhova, R. Wedell, *Part. Part. Syst. Charact.* 22 (2005) 384–390.
- [19] A. Knochel, G. Gaul, F. Lechtenberg, German patent DE 44441092C2, 1994.
- [20] Y.P. Feng, S.K. Sinha, H.W. Deckman, J.B. Hastings, D.P. Siddons, *Phys. Rev. Lett.* 71 (1993) 537–540.
- [21] S. Di Fonzo, W. Jark, S. Lagomarsin, C. Giannini, L. De Caro, A. Cedola, M. Muller, *Nature* 403 (2000) 638–641.
- [22] F. Pfeiffer, C. David, M. Burghammer, C. Riekkel, T. Salditt, *Science* 297 (2002) 230–234.
- [23] A.V. Baez, *J. Opt. Soc. Am.* 51 (1961) 405–412.
- [24] Y. Kagoshima, T. Ibuki, Y. Yokoyama, Y. Tsusaka, J. Matsui, K. Takai, M. Aino, *Jpn. J. Appl. Phys.* 40 (2001) L1190–L1192.
- [25] Y. Suzuki, A. Takeuchi, H. Takano, T. Ohigashi, H. Takenaka, *Jpn. J. Appl. Phys.* 40 (2001) 1508–1510.
- [26] Y. Kagoshima, Y. Yokoyama, T. Niimi, T. Koyama, Y. Tsusaka, J. Matsui, K. Takai, *J. Phys. IY (France)* 104 (2003) 49–52.
- [27] Y. Suzuki, M. Awaji, A. Takeuchi, H. Takano, K. Uesugi, Y. Komura, N. Kamijo, M. Yasumoto, S. Tamura, *J. Phys. IY (France)* 104 (2003) 35–40.
- [28] C. David, E. Ziegler, B. Nohammer, *J. Synchrotron Rad.* 8 (2001) 1054–1055.
- [29] B. Nohammer, C. David, M. Burghammer, C. Riekkel, *Appl. Phys. Lett.* 86 (2005) 163104.
- [30] B. Lai, W. Yun, D. Legnini, Y. Xiao, J. Chrzas, P.J. Viccaro, V. White, S. Bajikar, D. Denton, F. Cerrina, E.Di. Fabrizio, M. Gentilli, L. Grella, M. Baciocchi, *Appl. Phys. Lett.* 61 (1992) 1877–1879.
- [31] W. Yun, S.T. Pratt, R.M. Miller, Z. Cai, D.B. Hunter, A.G. Jarstfer, K.M. Kemner, B. Lai, H.R. Lee, D.G. Legnini, W. Rodrigues, C.I. Smith, *J. Synchrotron Rad.* 5 (1998) 1390–1395.

- [32] Z. Cai, B. Lai, Y. Xiao, S. Xu, J. Phys. IY (France) 104 (2003) 17–20.
- [33] I. Snigireva, A. Snigirev, G. Vaughan, M. Di Michiel, V. Kohn, V. Yunkin, M. Grigoriev, AIP Conf. Proc. 879 (2006) 998–1001.
- [34] D. Rudolph, G. Schmahl, B. Niemann, Proc. SPIE 316 (1982) 103–105.
- [35] N. Kamijo, Y. Suzuki, H. Takamo, M. Yasumoto, A. Takeuchi, M. Awaji, Rev. Sci. Instrum. 74 (2003) 5101–5104.
- [36] W. Yun, B. Lai, A.A. Krasnoperova, E. Di Fabrizio, Z. Cai, F. Cerina, Z. Chen, M. Gentili, E. Gluskin, Rev. Sci. Instrum. 70 (1999) 3537–3541.
- [37] E. Di Fabrizio, F. Romanato, M. Gentili, S. Cabrini, B. Kaulich, J. Susini, R. Barrett, Nature 401 (1999) 895–898.
- [38] H.C. Kang, G.B. Stephenson, C. Liu, R. Conley, A.T. Macrander, J. Maser, S. Bajt, H.N. Chapman, Appl. Phys. Lett. 86 (2005) 151109.
- [39] A. Snigirev, V. Kohn, I. Snigireva, B. Lengeler, Nature 384 (1996) 49–51.
- [40] A. Snigirev, V. Kohn, I. Snigireva, A. Souvorov, B. Lengeler, Appl. Opt. 37 (1998) 653–662.
- [41] P. Elleaume, Nucl. Instrum. Methods A 412 (1998) 483–506.
- [42] A. Chumakov, R. Ruffer, O. Leupold, A. Barla, H. Thiess, T. Asthalter, P. Doyle, A. Snigirev, A. Baron, Appl. Phys. Lett. 77 (2000) 31–33.
- [43] B. Lengeler, C.G. Schroer, M. Richwin, J. Tummler, M. Drakopoulos, A. Snigirev, I. Snigireva, Appl. Phys. Lett. 74 (1999) 3924–3926.
- [44] B. Lengeler, C. Schroer, J. Tummler, B. Benner, M. Richwin, A. Snigirev, I. Snigireva, M. Drakopoulos, J. Synchrotron Rad. 6 (1999) 1153–1167.
- [45] C. Schroer, F. Gunsler, B. Benner, M. Kuhlmann, J. Tummler, B. Lengeler, C. Rau, T. Weitkamp, A. Snigirev, I. Snigireva, Nucl. Instrum. Methods A 467–468 (2001) 966–969.
- [46] C.G. Schroer, J. Meyer, M. Kuhlmann, B. Benner, T.F. Gunsler, B. Lengeler, C. Rau, T. Weitkamp, A. Snigirev, I. Snigireva, Appl. Phys. Lett. 81 (2002) 1527–1529.
- [47] S. Engemann, H. Reichert, H. Dosch, J. Bilgram, V. Honimaki, A. Snigirev, Phys. Rev. Lett. 92 (2004) 205701.
- [48] B. Cederstrom, M. Lundqvist, C. Ribbing, Appl. Phys. Lett. 81 (2002) 1399–1401.
- [49] S.D. Shastri, J. Almer, C. Ribbing, B. Cederstrom, J. Synchrotron Rad. 14 (2007) 204–211.
- [50] M. Rossat, G. Vaughan, J. Wright, I. Snigireva, A. Snigirev, A. Bytchkov, C. Curfs, in press.
- [51] V. Aristov, M. Grigoriev, S. Kuznetsov, L. Shabelnikov, V. Yunkin, T. Weitkamp, C. Rau, I. Snigireva, A. Snigirev, M. Hoffmann, E. Voges, Appl. Phys. Lett. 77 (2000) 4058–4060.
- [52] I. Snigireva, A. Snigirev, C. Rau, T. Weitkamp, V. Aristov, M. Grigoriev, S. Kuznetsov, L. Shabelnikov, V. Yunkin, M. Hoffmann, E. Voges, Nucl. Instrum. Methods A 467–468 (2001) 982–985.
- [53] M. Drakopoulos, J. Zegenhagen, A. Snigirev, I. Snigireva, M. Hauser, K. Eberl, V. Aristov, L. Shabelnikov, V. Yunkin, Appl. Phys. Lett. 81 (2002) 2279–2281.
- [54] I. Snigireva, A. Snigirev, V. Yunkin, M. Drakopoulos, M. Grigoriev, S. Kuznetsov, M. Chukalina, M. Hoffmann, D. Nuesse, E. Voges, AIP Conf. Proc. 705 (2004) 708–712.
- [55] A. Snigirev, I. Snigireva, M. Grigoriev, V. Yunkin, M. Di Michiel, S. Kuznetsov, G. Vaughan, Proc. SPIE 6705 (2007) 670506-01.
- [56] A. Snigirev, I. Snigireva, M. Di Michiel, V. Honkimaki, M. Grigoriev, V. Nazmov, E. Reznikova, J. Mohr, V. Saile, Proc. SPIE 5539 (2004) 244–250.
- [57] C. Bergemann, H. Keymeulen, J.F. Van der Veen, Phys. Rev. Lett. 91 (2003) 204801.
- [58] C. Schroer, B. Lengeler, Phys. Rev. Lett. 94 (2005) 054802.
- [59] C.G. Schroer, Phys. Rev. B 74 (2006) 033405.
- [60] F. Pfeiffer, C. David, J.F. van der Veen, C. Bergemann, Phys. Rev. B 73 (2006) 245331.